"Precision measurement of annihilation point spread distributions for medically important positron emitters," S. E. Derenzo, in *Positron Annihilation*, R. R. Hasiguti and K. Fujiwara, Eds. Sendai, Japan: The Japan Institute of Metals, 1979, pp. 819-823.

PRECISION MEASUREMENT OF ANNIHILATION POINT SPREAD DISTRIBUTIONS FOR MEDICALLY IMPORTANT POSITRON EMITTERS

Stephen E. Derenzo
Donner Laboratory, University of California, Berkeley, California 94720

The range of positrons in tissue is the most important fundamental limit to the spatial resolution of positron imaging systems, especially when using the medically important positron emitters O-15, K-38, Zn-62, Ga-68, Rb-82, and I-122 whose beta end-points range from 1.7 to 3.4 MeV. While factors such as the intrinsic detector resolution and departures from 180° emission are well understood, the effect of positron range has not been as fully explored, either experimentally or theoretically. Several experiments have been performed to measure the distribution of annihilation points in water but the results are of limited accuracy since the detector resolution was comparable to the effect being measured.[1-3] The well known exponential relationship between positron transmission and absorber thickness is of questionable applicability here because it was derived from experiments that used distant absorbers rather than surrounding media[4,5] or did not distinguish between stopped and backscattered positrons[4].

To overcome these limitations, we designed an experiment using very thin sources in low density polyurethane foam to expand the annihilation point spread distributions by linear factors of 20 and 50. By placing the same sources in an aluminum cylinder, range effects are effectively suppressed and broadening from all other sources may be measured. Three positron sources were used: C-11, Ga-68 and Sr-82, having beta end-points of 0.96, 1.90, and 3.35 MeV respectively. The sources were evaporated from solutions of small volume and high specific activity and sealed between two 50 μm sheets of plastic 10 mm in diam. The sources were placed at the center of 50 cm diam cylinders of polyurethane foam of density 0.020 gm/cm^3 and 0.05 gm/cm^3 (including the density of trapped air). A typical foam cell had a volume of 1 mm^3 and 8 μm walls. Thus the absorber was homogeneous on the scale of the positron "range" and the observed distributions were 50-fold or 20-fold enlargements of those that occur in water or tissue. The projected distribution of annihilation points was measured using the Donner 280-Crystal Circular Positron Coincidence Tomograph[6]. This instrument measures the integral of positron annihilations between each of 14,700 detector pairs. These data are reorganized into 140 angles (1.29° spacing) of 105 parallel rays (5 mm spacing). See Fig. 1 for experimental set-up. The side shields were adjusted for a 15 mm gap to provide a section thickness having 7.5 mm FWHM, comparable to the resolution in the other two dimensions. The positron sources were placed at the center of the system with < 1 mm error and all angles were added together. The sum (after corrections for the known attenuation in the foam or aluminum) was the intensity function of the annihilation distribution projected onto a plane, hereafter called the point spread function (PSF). The measured PSF for the three sources in foam and metal are plotted in Figs. 2-4. The data for the sources in metal were used to estimate the effect of all sources of spatial broadening other than positron range. These include source size, detector size, deviations from 180° emission, and scattering in the foam or aluminum and lead shielding.

Let $p(r)$ be the PSF in foam and $f(r)$ the PSF in metal. If $q(r)$ is a PSF that includes the positron range effects only, then the observed $p(r)$ is a convolution of $q(r)$ and $f(r)$:

$$p(r) = \int_{-\infty}^{\infty} q(|r'|)\, f(|r-r'|)\, dr' \qquad (1)$$

We assume that f(r) has negligible broadening due to positron range and describes all other sources of experimental broadening in the projection measurements p(r).

The data in Figs. 2-4 suggest a sum of two exponentials and we found that a satisfactory fit could be obtained using the form:

$$q(r) = A\, e^{-r/r_1} + (1-A)\, e^{-r/r_2} \qquad (2)$$

The solid lines running through the data from the foam experiment in Figs. 2-4 were computed from Eq. (1) with the best fit values of A, r_1, and r_2 given in Table 1. The solid lines running through the aluminum data were drawn to guide the eye. Fig. 5 shows q(r) for all three isotopes drawn to the same horizontal scale.

Table 1. Summary of Results

Isotope	^{11}C	^{68}Ga	^{82}Sr
β^+ end point (MeV)	0.96(100%)	1.90(99%) 0.82(1.3%)	3.35(86%) 2.57(13%)
maximum practical range (mm)*	3.91	8.92	16.5
maximum practical range (mm)**	3.89	8.76	16.5
foam density used (gm/cm^3)	0.0201	0.0201	0.0503
observed PSF in foam:			
FWHM (mm)	7	8	9
FW(0.1)M (mm)	29	100	64
observed PSF in aluminum:			
FWHM (mm)	6	6	6
FW(0.1)M (mm)	13	13	13
best fit parameters:†			
A	0.916	0.811	0.898
r_1 (mm)††	0.078	0.162	0.301
r_2 (mm)††	0.457	1.15	2.99
best fit q(r):††			
FWHM (mm)	0.12	0.30	0.48
FW(0.1)M (mm)	0.46	1.6	2.1
rms (mm)	0.38	1.2	2.8
r(mm) for u(r)=0.5§	0.54	1.6	4.3
r(mm) for u(r)=0.75§	1.03	2.7	6.9
r(mm) for u(r)=0.90§	1.6	3.7	9.5

* calculated as mm water equivalent from the β^+ end point and ref. 7.
**calculated as mm water equivalent from the β^+ end point and ref. 8.
† parameters in eqn. 2 that give the best fit of eqn.1 to the measured projections in foam (figs. 2-4).
††multiplied by density of foam to give mm water equivalent.
§ u(r) is the fraction of annihilation points that project onto a plane within a circle of radius r (eqn. 3).

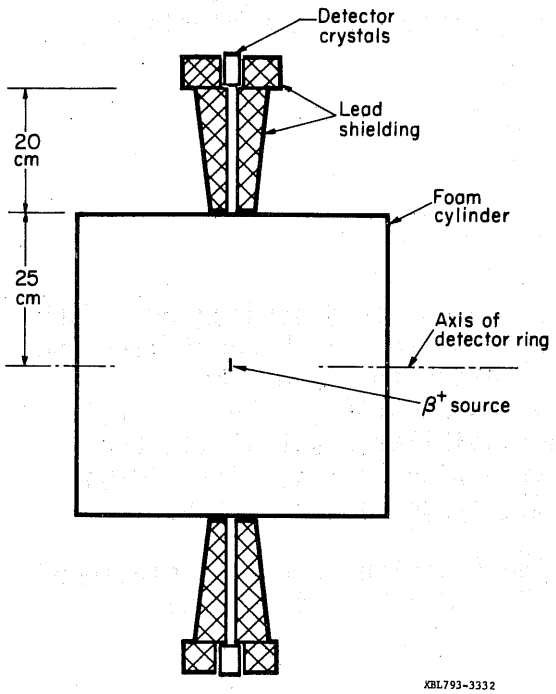

Fig. 1. Donner Laboratory 280-Crystal Positron Tomograph as used to measure the distribution of annihilation points in foam.

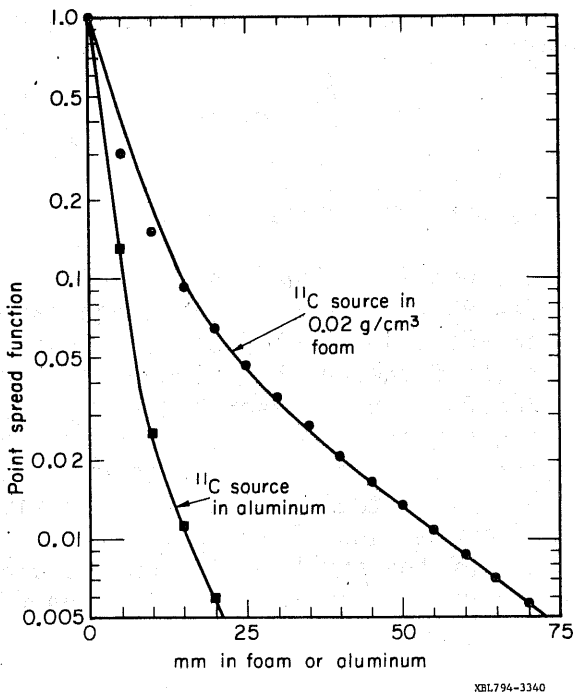

Fig. 2. C-11 in foam and aluminum. (Beta end-point 0.96 MeV.)

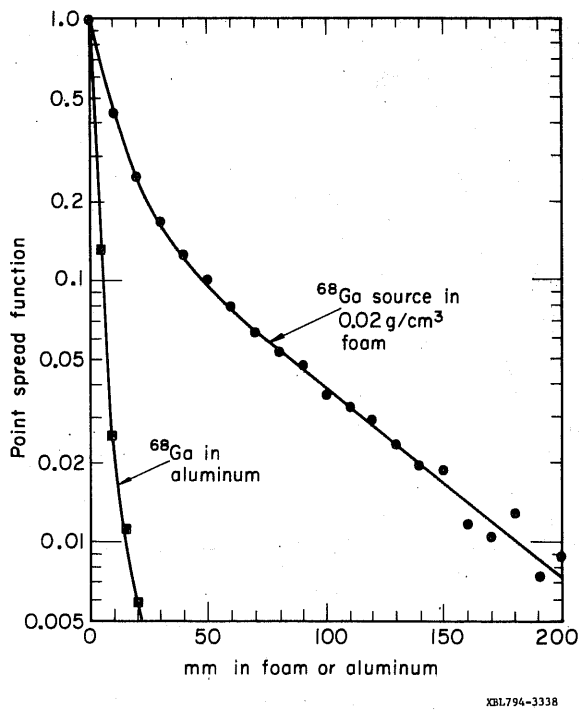

Fig. 3. Ga-68 in foam and aluminum. (Beta end-point 1.90 MeV.)

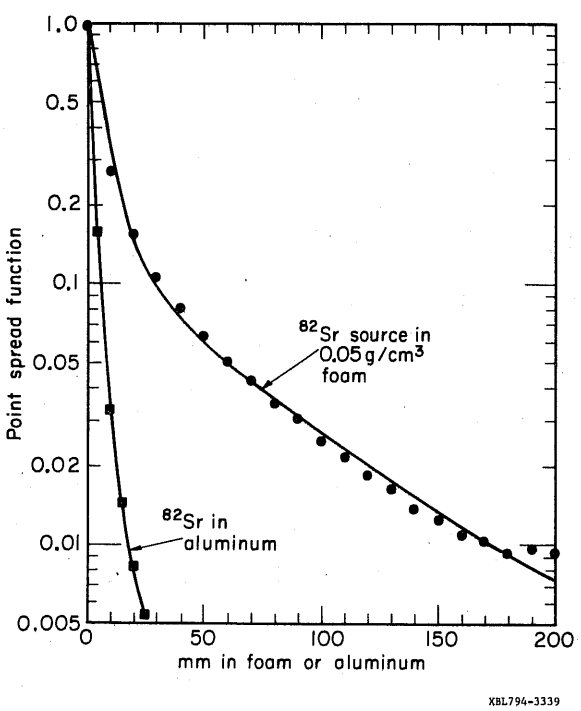

Fig. 4. Sr-82 in foam and aluminum. (Beta end-point 3.35 MeV.)

It is of interest (especially for area detectors) to compute the fraction u(r) of annihilations that project onto a plane within a circle of radius r:

$$u(r) = \int_0^r q(r')\, r'\, dr' \Big/ \int_0^\infty q(r')\, r'\, dr' \qquad (3)$$

The results are plotted in Fig. 6.

A synopsis of the results follows:

(1) The PSF due to positron range cannot be adequately described by a FWHM or FW(0.1)M. The distribution is sharply peaked, has broad tails, and most of the annihilation points project beyond the FW(0.1)M.

(2) The PSF can be described by a sum of two exponentials. The first is associated with a small fraction of the annihilations that cluster near the origin. The second is associated with the majority of annihilations that lie in the extensive tails of the distribution. (Compare Figs. 5 and 6).

(3) 50% of the annihilation points project onto a plane within a circle of radius 0.54 mm for C-11, 1.6 mm for Ga-68 and 4.3 mm for Rb-82.

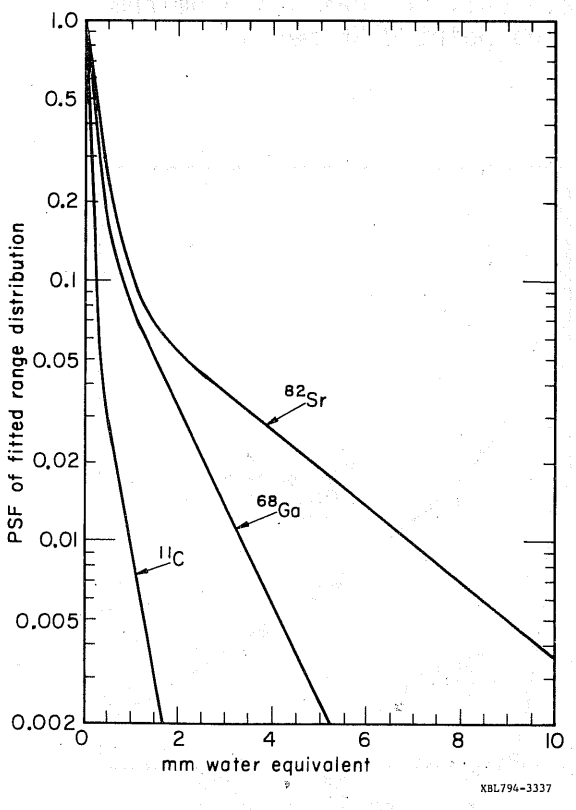

Fig. 5. Best fit q(r) (see Eq. 2) to the data of Figs. 2-4, showing the point spread due to range only.

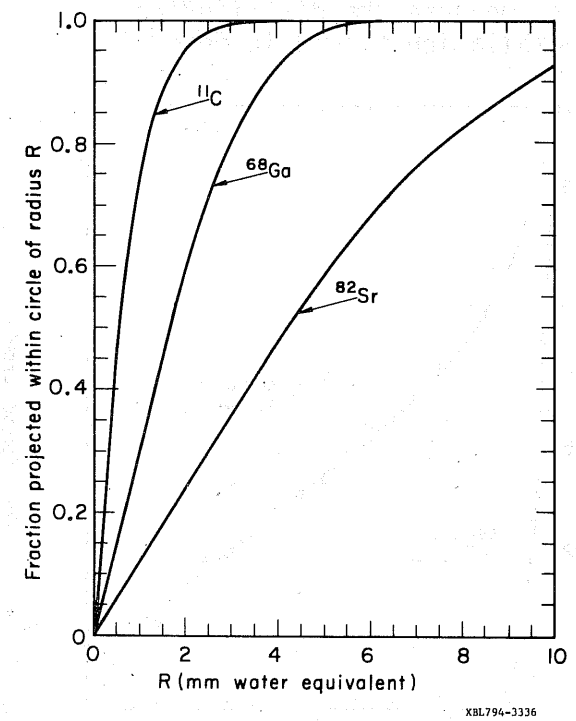

Fig. 6. Fraction of projected annihilations occurring within a circle of radius R, computed from best fit q(R) and Eq. (3).

Acknowledgments

I wish to thank Drs. T. F. Budinger and R. H. Huesman for many valuable discussions, T. Vuletich for invaluable technical contributions, Y. Yano for providing isotopes of high specific sensitivity, and H. A. O'Brien, Jr. of Los Alamos Scientific Laboratory for supplying the necessary Sr-82. This work was supported by the Division of Biomedical and Environmental Research of the U.S. Department of Energy.

References

1. Cho, Z.H., J.K. Chan, L. Eriksson, M. Singh, L.S. Graham and Y. Yano. Positron Ranges Obtained from Biomedically Important Positron Emitting Radionuclides. J. Nucl. Med. 16:1174-1176, 1975.

2. Phelps, M.E., E.J. Hoffman, S.C. Huang and M.M. Ter-Pogossian. Effect of Positron Range on Spatial Resolution. J. Nucl. Med. 16:649-652, 1975.

3. Llacer, J. and L.S. Graham. The Effect of Improving Energy Resolution on Gamma Camera Performance: A Quantitative Analysis. IEEE Trans. Nucl. Sci. NS-22(1):309-343, 1975.

4. Evans, R.D. The Atomic Nucleus. McGraw-Hill, New York, 1955, pp. 621-628.

5. Brandt, W. and R. Paulin. Positron Implantation - Profile Effects in Solids. Phys. Rev. B15:2511-2518, 1977.

6. Derenzo, S.E., T.F. Budinger, J.L. Cahoon, W.L. Greenberg, R.H. Huesman and T. Vuletich. The Donner 280-Crystal High Resolution Positron Tomograph. IEEE Trans. Nucl. Sci., to be published 1979. Also see the accompanying paper in this volume. The C-11, Ga-68 and Sr-82 source strengths were 38 μCi, 3.3 μCi and 15 μCi, and the event rates were 1020/sec, 25/sec and 112/sec, respectively.

7. Katz, L. and A.S. Penfold. Range-Energy Relations for Electrons and the Determination of Beta-Ray End-Point Energies by Absorption. Rev. Mod. Phys. 24:28-44, 1952.

8. Kobetich, E.J. and R. Katz. Energy Deposition by Electron Beam δ Rays. Phys. Rev. 170:391-396, 1968.